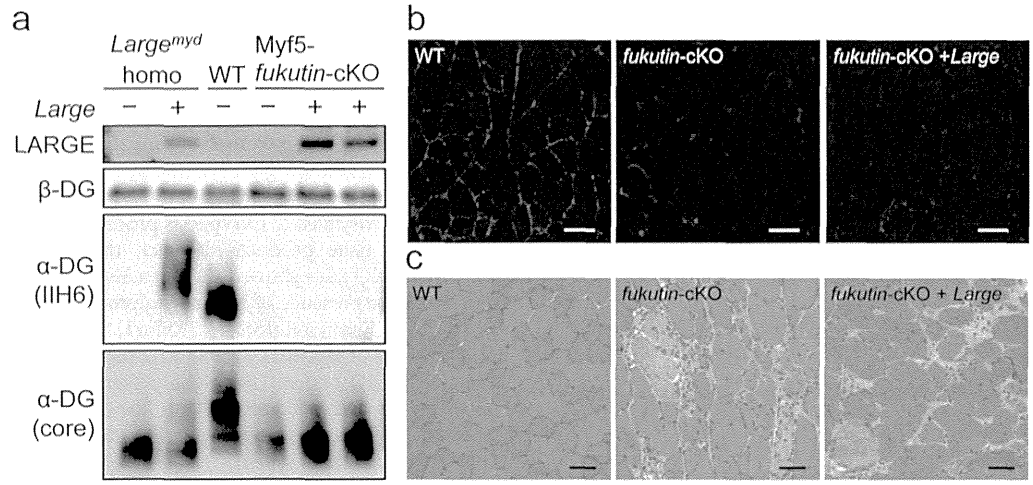

Figure 3 | Systemic gene transfer of Large into Myf5-fukutin cKO mice after onset. AAV9-MCK-*Large* was administered to 4-week-old Myf5-*fukutin* cKO mice via tail vein injection; after 2 months, the skeletal muscles were harvested and analysed for α-DG glycosylation (a, b) and histology (c). Although LARGE was expressed (a), the levels of α-DG glycosylation were unchanged in AAV-treated Myf5-*fukutin*-cKO mice (a, b). H&E staining for the tibialis anterior muscle did not show improvement of the muscular dystrophic phenotype of Myf5-*fukutin*-cKO mice (c). WT, litter control mice (*fukutin*$^{lox/lox}$ without cre-transgene); *fukutin*-cKO, untreated Myf5-*fukutin*-cKO mice; and *fukutin* cKO + *Large*, Myf5-*fukutin*-cKO mice with AAV9-MCK-*Large* treatment. Bar = 50 μm. The full-length blots with α-DG (IIH6), α-DG (core), LARGE, and β-DG are presented in Supplementary Figure S2e-h, respectively.

Sangyo Co. Ltd., Tokyo); 20% of the top and bottom values were excluded to obtain the mean. Statistical analysis was performed to determine means and s.e.m.; *P*-values <0.05 were considered significant (Mann–Whitney U test).

Antibodies. Antibodies for western blotting and immunofluorescence were as follows: mouse monoclonal antibody 8D5 against β-DG (Novocastra); mouse monoclonal antibody IIH6 against α-DG (Millipore); rat monoclonal antibody against mouse F4/80 (BioLegend); rabbit polyclonal antibody against collagen I (AbD Serotec); mouse monoclonal antibody against FLAG tag (Sigma); and rabbit polyclonal antibody against c-Myc tag (Santa Cruz). Rabbit polyclonal antibody against LARGE was raised using recombinant human LARGE protein expressed in *E. coli*. Antisera were purified by Melon gel IgG purification kit (Pierce). Rat monoclonal antibody against the α-DG core protein (3D7) was generated from a α-DG-Fc fusion protein[52].

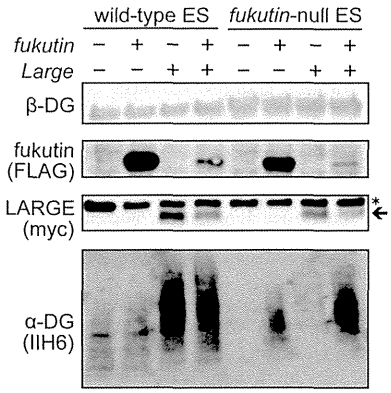

Figure 4 | α-DG glycosylation in fukutin-null ES cells after fukutin or LARGE expression. Fukutin (FLAG-tagged) and/or LARGE (myc-tagged) were expressed in wild-type or *fukutin*-null mouse ES cells and α-DG glycosylation status was analysed by western blotting. Exogenous LARGE expression produced highly glycosylated α-DG in wild-type but not *fukutin*-null ES cells, indicated by IIH6 staining. Co-transfection of *fukutin* and *Large* yielded LARGE-dependent glycosylation of α-DG in *fukutin*-null ES cells. Arrow and asterisk indicate LARGE protein and non-specific signals, respectively. The full-length blots with α-DG (IIH6), LARGE (myc), fukutin (FLAG), and β-DG are presented in Supplementary Figure S2i-l, respectively.

Protein preparation and western blotting. DG was enriched from solubilized skeletal muscle as described[27]. Briefly, skeletal muscles (TA ~30 mg, calf ~100 mg) were solubilised in Tris-buffered saline containing 1% Triton X-100 and protease inhibitors (Nacalai). The solubilised fraction was incubated with wheat germ agglutinin (WGA)-agarose beads (Vector Laboratories) at 4°C for 16 h; DG was eluted with SDS-PAGE loading buffer. To detect LARGE protein expression, total lysates were analysed by western blotting. Proteins were separated in 4–15% linear gradient SDS gels, then transferred to polyvinylidene fluoride (PVDF) membranes (Millipore). Blots were probed with antibodies and developed with horseradish peroxidase (HRP)-enhanced chemiluminescence reagent (Supersignal West Pico, Pierce; or ECL Prime, GE Healthcare).

Histology and immunofluorescence analysis. For H&E staining, cryosections (7 μm) were stained for 2 min in haematoxylin, 1 min in eosin, and dehydrated with ethanol and xylene. IIH6-immunofluorescence analysis was performed after treating the with cold ethanol/acetic acid (1 : 1) for 1 min, blocking with 5% goat serum in MOM Mouse Ig Blocking Reagent (Vector Laboratories) at room temperature for 1 h, and incubation with primary antibodies diluted in MOM Diluent (Vector Laboratories) overnight at 4°C. For F4/80- and collagen I-immunofluorescence, sections were blocked with 3% bovine serum albumin (BSA) in phosphate-buffered saline (PBS) at room temperature for 1 h, and then with primary antibodies diluted in 1% BSA overnight at 4°C. The slides were washed with PBS and incubated with Alexa Fluor 488-conjugated or Alexa Fluor 555-conjugated secondary antibodies (Molecular Probes) at room temperature for 30 min. Permount (Fisher Scientific) and TISSU MOUNT (Shiraimatsu Kikai) were used for H&E staining and immunofluorescence, respectively. Sections were observed by fluorescence microscopy (Leica DMR, Leica Microsystems).

ES cell culture. ES cells were cultured in DMEM with 20% heat-inactivated foetal bovine serum, 100 μM 2-mercaptoethanol, 1 mM non-essential amino acids (Gibco), 2 mM L-glutamine (Nacalai), and 10^3 U/mL leukaemia inhibitory factor (Millipore). Targeted disruptions of the *fukutin* gene in ES cells have been described previously[53]. Transfection was performed with Lipofectamine LTX reagents (Invitrogen) according to manufacturer protocols. After 48 h transfection, cells were lysed with Tris-buffered saline containing 1% Triton X-100 and protease inhibitors (Nacalai). DG proteins were enriched with WGA-beads and analysed by western blotting.

1. Toda, T. *et al.* Fukuyama-type congenital muscular dystrophy (FCMD) and alpha-dystroglycanopathy. *Congenit. Anom. (Kyoto).* **43**, 97–104 (2003).
2. Michele, D. E. & Campbell, K. P. Dystrophin-glycoprotein complex: post-translational processing and dystroglycan function. *J. Biol. Chem.* **278**, 15457–15460 (2003).
3. Beltrán-Valero de Bernabé, D. *et al.* Mutations in the O-mannosyltransferase gene POMT1 give rise to the severe neuronal migration disorder Walker-Warburg syndrome. *Am. J. Hum. Genet.* **71**, 1033–1043 (2002).

4. van Reeuwijk, J. *et al.* POMT2 mutations cause alpha-dystroglycan hypoglycosylation and Walker-Warburg syndrome. *J. Med. Genet.* **42**, 907–912 (2005).
5. Yoshida, A. *et al.* Muscular dystrophy and neuronal migration disorder caused by mutations in a glycosyltransferase, POMGnT1. *Dev. Cell* **1**, 717–724 (2001).
6. Kobayashi, K. *et al.* An ancient retrotransposal insertion causes Fukuyama-type congenital muscular dystrophy. *Nature* **394**, 388–392 (1998).
7. Brockington, M. *et al.* Mutations in the fukutin-related protein gene (FKRP) cause a form of congenital muscular dystrophy with secondary laminin alpha2 deficiency and abnormal glycosylation of alpha-dystroglycan. *Am. J. Hum. Genet.* **69**, 1198–1209 (2001).
8. Longman, C. *et al.* Mutations in the human LARGE gene cause MDC1D, a novel form of congenital muscular dystrophy with severe mental retardation and abnormal glycosylation of alpha-dystroglycan. *Hum. Mol. Genet.* **12**, 2853–2861 (2003).
9. Willer, T. *et al.* ISPD loss-of-function mutations disrupt dystroglycan O-mannosylation and cause Walker-Warburg syndrome. *Nat. Genet.* **44**, 575–580 (2012).
10. Roscioli, T. *et al.* Mutations in ISPD cause Walker-Warburg syndrome and defective glycosylation of α-dystroglycan. *Nat. Genet.* **44**, 581–585 (2012).
11. Manzini, M. C. *et al.* Exome sequencing and functional validation in zebrafish identify GTDC2 mutations as a cause of Walker-Warburg syndrome. *Am. J. Hum. Genet.* **91**, 541–517 (2012).
12. Hara, Y. *et al.* A dystroglycan mutation associated with limb-girdle muscular dystrophy. *N. Engl. J. Med.* **364**, 939–946 (2011).
13. Vuillaumier-Barrot, S. *et al.* Identification of mutations in TMEM5 and ISPD as a cause of severe cobblestone lissencephaly. *Am. J. Hum. Genet.* **91**, 1135–1143 (2012).
14. Jae, L. T. *et al.* Deciphering the glycosylome of dystroglycanopathies using haploid screens for lassa virus entry. *Science* **340**, 479–483 (2013).
15. Stevens, E. *et al.* Mutations in B3GALNT2 cause congenital muscular dystrophy and hypoglycosylation of α-dystroglycan. *Am. J. Hum. Genet.* **92**, 354–365 (2013).
16. Buysse, K. *et al.* Missense mutations in β-1,3-N-acetylglucosaminyltransferase 1 (B3GNT1) cause Walker-Warburg syndrome. *Hum. Mol. Genet.* **22**, 1746–1754 (2013).
17. Carss, K. J. *et al.* Mutations in GDP-mannose pyrophosphorylase B cause congenital and limb-girdle muscular dystrophies associated with hypoglycosylation of α-dystroglycan. *Am. J. Hum. Genet.* **93**, 29–41 (2013).
18. Lefeber, D. J. *et al.* Autosomal recessive dilated cardiomyopathy due to DOLK mutations results from abnormal dystroglycan O-mannosylation. *PLoS Genet.* **7**, e1002427 (2011).
19. Yang, A. C. *et al.* Congenital disorder of glycosylation due to DPM1 mutations presenting with dystroglycanopathy-type congenital muscular dystrophy. *Mol. Genet. Metab.* **110**, 345–351 (2013).
20. Barone, R. *et al.* DPM2-CDG: a muscular dystrophy-dystroglycanopathy syndrome with severe epilepsy. *Ann. Neurol.* **72**, 550–558 (2012).
21. Lefeber, D. J. *et al.* Deficiency of Dol-P-Man synthase subunit DPM3 bridges the congenital disorders of glycosylation with the dystroglycanopathies. *Am. J. Hum. Genet.* **85**, 76–86 (2009).
22. Kanagawa, M. Dystroglycan glycosylation and its involvement in muscular dystrophy. *Trends Glycosci. Glycotech.* **26**, 41–57 (2014).
23. Barresi, R. & Campbell, K. P. Dystroglycan: from biosynthesis to pathogenesis of human disease. *J. Cell Sci.* **119**, 199–207 (2006).
24. Yoshida-Moriguchi, T. *et al.* O-mannosyl phosphorylation of alpha-dystroglycan is required for laminin binding. *Science* **327**, 88–92 (2010).
25. Michele, D. E. *et al.* Post-translational disruption of dystroglycan-ligand interactions in congenital muscular dystrophies. *Nature* **418**, 417–422 (2002).
26. Han, R. *et al.* Basal lamina strengthens cell membrane integrity via the laminin G domain-binding motif of alpha-dystroglycan. *Proc. Natl. Acad. Sci. USA.* **106**, 12573–12579 (2009).
27. Kanagawa, M. *et al.* Impaired viability of muscle precursor cells in muscular dystrophy with glycosylation defects and amelioration of its severe phenotype by limited gene expression. *Hum. Mol. Genet.* **22**, 3003–3015 (2013).
28. Godfrey, C. *et al.* Refining genotype phenotype correlations in muscular dystrophies with defective glycosylation of dystroglycan. *Brain* **130**, 2725–2735 (2007).
29. Godfrey, C., Foley, A. R.., Clement, E. & Muntoni, F. Dystroglycanopathies: coming into focus. *Curr. Opin. Genet. Dev.* **21**, 278–285 (2011).
30. Murakami, T. *et al.* Fukutin gene mutations cause dilated cardiomyopathy with minimal muscle weakness. *Ann. Neurol.* **60**, 597–602 (2006).
31. Hayashi, Y. K. *et al.* Selective deficiency of alpha-dystroglycan in Fukuyama-type congenital muscular dystrophy. *Neurology* **57**, 115–121 (2001).
32. Fukuyama, Y., Osawa, M. & Suzuki, H. Congenital progressive muscular dystrophy of the Fukuyama type - clinical, genetic and pathological considerations. *Brain Dev.* **3**, 1–29 (1981).
33. Toda, T., Kobayashi, K., Kondo-Iida, E., Sasaki, J. & Nakamura, Y. The Fukuyama congenital muscular dystrophy story. *Neuromuscul. Disord.* **10**, 153–159 (2000).
34. Kuga, A. *et al.* Absence of post-phosphoryl modification in dystroglycanopathy mouse models and wild-type tissues expressing non-laminin binding form of α-dystroglycan. *J. Biol. Chem.* **287**, 9560–9567 (2012).
35. Inamori, K. *et al.* Dystroglycan function requires xylosyl- and glucuronyltransferase activities of LARGE. *Science* **335**, 93–96 (2012).
36. Goddeeris, M. M. *et al.* LARGE glycans on dystroglycan function as a tunable matrix scaffold to prevent dystrophy. *Nature* **503**, 136–140 (2013).
37. Barresi, R. *et al.* LARGE can functionally bypass alpha-dystroglycan glycosylation defects in distinct congenital muscular dystrophies. *Nat. Med.* **10**, 696–703 (2004).
38. Yu, M. *et al.* Adeno-associated viral-mediated LARGE gene therapy rescues the muscular dystrophic phenotype in mouse models of dystroglycanopathy. *Hum. Gene Ther.* **24**, 317–330 (2013).
39. Vannoy, C. H. *et al.* Adeno-associated virus-mediated overexpression of LARGE rescues α-dystroglycan function in dystrophic mice with mutations in the fukutin-related protein. *Hum. Gene. Ther. Methods.* **25**, 187–196 (2014).
40. Yagi, H. *et al.* AGO61-dependent GlcNAc modification primes the formation of functional glycans on α-dystroglycan. *Sci. Rep.* **3**, 3288 (2013).
41. Whitmore, C. *et al.* The transgenic expression of LARGE exacerbates the muscle phenotype of dystroglycanopathy mice. *Hum. Mol. Genet.* **23**, 1842–1855 (2014).
42. Saito, F. *et al.* Overexpression of LARGE suppresses muscle regeneration via down-regulation of insulin-like growth factor 1 and aggravates muscular dystrophy in mice. *Hum. Mol. Genet.* **23**, 4543–4558 (2014).
43. Gumerson, J. D. *et al.* Muscle-specific expression of LARGE restores neuromuscular transmission deficits in dystrophic LARGE(myd) mice. *Hum. Mol. Genet.* **22**, 757–768 (2013).
44. Yoshida-Moriguchi, T. *et al.* SGK196 is a glycosylation-specific O-mannose kinase required for dystroglycan function. *Science* **341**, 896–899 (2013).
45. Taniguchi-Ikeda, M. *et al.* Pathogenic exon-trapping by SVA retrotransposon and rescue in Fukuyama muscular dystrophy. *Nature* **478**, 127–131 (2011).
46. Kanagawa, M. *et al.* Residual laminin-binding activity and enhanced dystroglycan glycosylation by LARGE in novel model mice to dystroglycanopathy. *Hum. Mol. Genet.* **18**, 621–631 (2009).
47. Foust, K. D. *et al.* Intravascular AAV9 preferentially targets neonatal neurons and adult astrocytes. *Nat. Biotechnol.* **27**, 59–65 (2009).
48. Nakano, I., Funahashi, M., Takada, K. & Toda, T. Are breaches in the glia limitans the primary cause of the micropolygyria in Fukuyama-type congenital muscular dystrophy (FCMD)? Pathological study of the cerebral cortex of an FCMD fetus. *Acta. Neuropathol.* **91**, 313–321 (1996).
49. Chiyonobu, T. *et al.* Effects of fukutin deficiency in the developing mouse brain. *Neuromuscul. Disord.* **15**, 416–426 (2005).
50. Okada, T. *et al.* Scalable purification of adeno-associated virus serotype 1 (AAV1) and AAV8 vectors, using dual ion-exchange adsorptive membranes. *Hum. Gene Ther.* **20**, 1013–1021 (2009).
51. Yuasa, K. *et al.* Adeno-associated virus vector-mediated gene transfer into dystrophin-deficient skeletal muscles evokes enhanced immune response against the transgene product. *Gene Ther.* **9**, 1576–1588 (2002).
52. Kanagawa, M. *et al.* Post-translational maturation of dystroglycan is necessary for pikachurin binding and ribbon synaptic localization. *J. Biol. Chem.* **285**, 31208–31216 (2010).
53. Takeda, S. *et al.* Fukutin is required for maintenance of muscle integrity, cortical histiogenesis and normal eye development. *Hum. Mol. Genet.* **12**, 1449–1459 (2003).

Acknowledgments

We would like to thank the past and present members of Dr. Toda's laboratory for fruitful discussions and scientific contributions. We also thank Hiromi Hayashita-Kinoh for providing technical support. This work was supported by the Ministry of Health, Labour, and Welfare of Japan [Intramural Research Grant for Neurological and Psychiatric Disorders of National Centre of Neurology and Psychiatry (26-8)]; the Ministry of Education, Culture, Sports, Science and Technology of Japan [a Grant-in-Aid for Scientific Research (A) 26253057 to T.T.; a Grant-in-Aid for Young Scientists (A) 24687017 to M.K.; and a Grant-in-Aid for Scientific Research on Innovative Areas (Deciphering sugar chain-based signals regulating integrative neuronal functions) 24110508 to M.K.]; a Senri Life Science Foundation grant to M.K.; and a Takeda Science Foundation grant to M.K.

Author contributions

Y.O., M.K., T.O., K.K., S.T. and T.T. conceived and designed the research. Y.O., M.K. and C.I. performed experiments and analysed the data. C.Y., K.K., T.C. and T.O. constructed the AAV vectors. Y.O., M.K. and T.T. wrote the paper. All authors reviewed the manuscript.

Additional information

Supplementary information accompanies this paper at http://www.nature.com/scientificreports

Competing financial interests: The authors declare no competing financial interests.

How to cite this article: Ohtsuka, Y. *et al.* Fukutin is prerequisite to ameliorate muscular dystrophic phenotype by myofiber-selective LARGE expression. *Sci. Rep.* **5**, 8316; DOI:10.1038/srep08316 (2015).

筋ジストロフィー治療の新しい展開

戸田　達史

要　旨

最も多いDuchenne型筋ジストロフィー(Duchenne muscular dystrophy：DMD)原因遺伝子ジストロフィンのクローニングを契機として，これまでに様々な筋ジストロフィーの原因遺伝子が同定されている．Disease-modifying therapyの開発が期待されており，現在臨床治験段階にあるエクソン・スキップ治療とリードスルー治療を中心に，将来臨床応用が期待されている分子標的治療の開発の現状について紹介する．福山型筋ジストロフィーは筋と脳を侵す日本に多い常染色体性劣性遺伝性疾患である．我々は原因遺伝子を同定，原因蛋白質をフクチンと命名した．患者ではフクチン遺伝子の3'非翻訳領域にSVA型レトロトランスポゾンの挿入を認めるが，本症がスプライシング異常症であることを見出し，これを制御するアンチセンス核酸を用い，患者細胞およびモデルマウスでの治療に成功した．この治療法は全ての患者に適応となる初の根治療法となる可能性があり，臨床応用を目指す．

〔日内会誌　103：2820～2828，2014〕

Key words　Duchenne型筋ジストロフィー，エクソンスキッピング，アンチセンス治療，リードスルー治療，福山型筋ジストロフィー

はじめに

筋ジストロフィーは，骨格筋線維の変性・壊死と不完全再生のサイクルを繰り返しながら間質の線維化・脂肪化が進行する遺伝性疾患群である．臨床的には進行性の骨格筋萎縮と筋力低下を呈しADLが低下するだけでなく，呼吸筋不全や心不全といった重篤な合併症を併発することもある難病である．新聞などを通し，または一般人の感覚で筋ジストロフィーというと，1個の疾患のように感じられるかもしれない．しかし，表に見るように筋ジストロフィーは遺伝形式も症状も遺伝子も異なる40種以上からなる疾患群であり，うちDuchenne型，肢帯型，顔面肩甲上腕型，先天型(福山型)，筋強直型，遠位型などが代表的である．

最も多いDuchenne型筋ジストロフィー(Duchenne muscular dystrophy：DMD)の原因遺伝子ジストロフィンのクローニングを契機として，これまでに様々な筋ジストロフィーの責任遺伝子が同定されているが，現在も治療の中心は対症療法である．リハビリテーション，心不全に対する薬物療法，呼吸筋麻痺に対する呼吸管理により，生命予後は約10年延長したといわれる．唯一エビデンスのある薬物療法は副腎

神戸大学大学院医学研究科神経内科学/分子脳科学

The Cutting-edge of Medicine ; Recent development of therapy for muscular dystrophy.

Tatsushi Toda : Division of Neurology/Molecular Brain Science, Kobe University Graduate School of Medicine, Japan.

表

疾患名	遺伝形式	遺伝子座	シンボル名	遺伝子産物
Duchenne型	XR（x劣性）	Xp21.2	DMD	ジストロフィン
Becker型	XR	Xp21.2	DMD	ジストロフィン
Emery-Dreifuss型	XR	Xq28	EMD	エメリン
	AD	1q11-23	EDMD-AD	ラミンA/C
肢帯型（1型）	AD（常染色体優性）	5q31	LGMD1A	ミオチリン
	AD	1q11-21	LGMD1B	ラミンA/C
	AD	3p25	LGMD1C	カベオリン3
肢帯型（2型）	AR（常染色体劣性）	15q15.1-21.1	LGMD2A	カルパイン3
	AR	2p13	LGMD2B	ジスフェルリン
	AR	13q12	LGMD2C	γサルコグリカン
	AR	17q12-21	LGMD2D	αサルコグリカン
	AR	4q12	LGMD2E	βサルコグリカン
	AR	5q33-34	LGMD2F	δサルコグリカン
	AR	17q11-12	LGMD2G	テレソニン
	AR	9q31-34.1	LGMD2H	TRIM32
	AR	19q13.3	LGMD2I	FKRP
顔面肩甲上腕型	AD	4q35	FSHD	?
先天性（メロシン欠損型）	AR	6q2	MDC1A	ラミニンα2
先天性（福山型）	AR	9q31	FCMD	フクチン
先天性（muscle-eye-brain病）	AR	1p33-34	MEB	POMGnT1
先天性（Walker-Warburg症候群）	AR	9q34	WWS	POMT1
先天性（インテグリン欠損型）	AR	12q	?	インテグリンα7
先天性（rigid-spine型）	AR	1p3	RSMD1	SEPN1
先天性（その他）	AR	19q13.3	MDC1C	FKRP
筋強直性	AD	19q13	DM	ミオトニンキナーゼ
	AD	3q21	DM2	ZNF9
遠位型（三好型）	AR	2p12-14	MM	ジスフェルリン
遠位型（rimmed-vacuole型）	AR	9p1-q1	DMRV	GNE
遠位型（家族性封入体型）	AR	9p1-q1	HIBM	GNE
眼咽頭型	AD	14q11.2-13	OPMD	ポリA結合蛋白2
表皮水疱症型	AR	8q24-qter	MD-EBS	プレクチン
デスミン関連型	AD/AR	2q35	DES	デスミン

皮質ステロイド薬の内服であるが，治療効果は限られており，より有効なdisease-modifying therapyの開発が期待されている．ここでは最近のトピックスとして，現在臨床治験段階にあるエクソン・スキップ治療とリードスルー治療を中心に，将来臨床応用が期待されている分子標的治療の開発の現状について紹介するとともに，筆者らが主導する日本に特異的に多い福山型筋ジストロフィーが治療可能かもしれないことを解説する．

1．筋ジストロフィーの臨床治験段階にある治療

1）エクソン・スキップ治療

DMDの責任遺伝子であるジストロフィン遺伝子はX染色体短腕上Xp21.1に存在する巨大な遺伝子であり，79個のエクソンからなる．ジストロフィン異常症の遺伝子異常はエクソン単位の欠失が70～80%，ナンセンス変異などの微小変

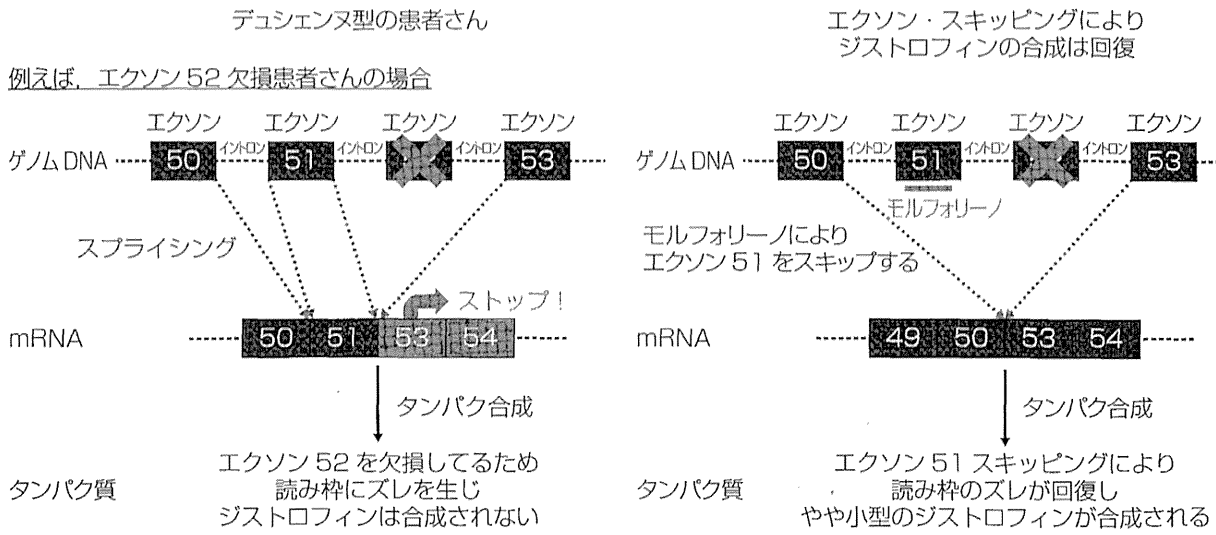

図1．アンチセンス核酸によるエクソンスキッピング
筋ジス犬が走り出す．Duchenne患者治験中．

異が20%とされている．同じジストロフィン遺伝子の欠失であるにも関わらず，DMDとBecker型筋ジストロフィー(Becker type muscular dystrophy：BMD)で重症度に違いがあるのは，フレームシフト則により説明される．すなわち，欠失エクソンの総塩基数が3の倍数であれば翻訳の際の読み枠は維持され（in-frame欠失），機能を有する少し短くなったジストロフィン蛋白が合成されるため軽症のBMDとなるのに対して，3の倍数でなければ読み枠にずれが生じ(out-of-frame欠失)，未熟終始コドンの出現によりジストロフィン蛋白が合成されないため重症のDMDとなる．このフレームシフト則に基づいて，アンチセンス核酸化合物により欠失エクソンに隣接するエクソンをスプライシングの過程でスキップさせ，mRNAレベルでの欠失を3の倍数にして読み枠を修正し，DMDを軽症化しようとするのが，エクソン・スキップ治療である（図1）．

現在，スキッピングの標的とされているのはエクソン51で，欠失によるDMD患者の約10%が治療対象となる．エクソン・スキップを誘導するアンチセンス核酸化合物としては，低毒性でヌクレアーゼ耐性の安定な人工核酸である2'-O-methyl oligonucleotide（2OMeAS）とphosphorodiamidate morpholino oligomer（PMO）が用いられている．Prosensa Therapeutics社が開発しているPRO051（drisapersen®）は前者の，またSarepta社のAVI-4658（eteplirsen®）は後者の化合物である．2011年これら2剤について欧米で第2相の臨床治験の結果が報告された[1,2]．両者ともエクソン51スキップの誘導とジストロフィン蛋白発現の回復が確認され，安全性にも問題がなかった．PRO051はグラキソ社が第3相国際共同治験を行い，2013年10月残念ながら患者の6分間歩行に有意な改善が認められなかったため，現在グループ化してサブ解析中である．

また，2012年9月Sarepta社はeteplirsenの治験において，6分間歩行テストの改善データを公表した．50 mg/kg投与群の4名のDMD患児では投与後48週の時点で歩行距離が21 m延長したのに対して，プラセボで開始し24週目から実薬を投与された遅延開始群では36週の時点で歩行距離は−78 mまで減少した．48週時点では−68 mまで回復したが，早期開始群との間に89 mという有意差がついた．症例数は少ないが，この成績はエクソン・スキップ治療に期待を抱かせる．

また，日本ではエクソン53スキップの医師主導治験が2013年開始された．

2）リードスルー治療

点変異により終始コドンが生じると，蛋白質が合成されず欠損症状を呈する．こうしたナンセンス変異はDMD患者の約15％を占めるとされているが，その場合の治療戦略としてリードスルー治療が考えられる．すなわち，薬物を用いて翻訳過程で終始コドンを読み飛ばす（リードスルー）ことにより，蛋白発現を回復させようという試みである．アミノグリコシド系抗生物質は，真核細胞においてもmRNAの翻訳忠実度を低下させ，時として終始コドンを読み越えさせることが知られていた．DMDのモデル動物である*mdx*マウスはジストロフィン遺伝子のナンセンス変異を持つが，Sweeneyらは*mdx*マウスにゲンタマイシンを投与して，ジストロフィン蛋白発現の回復と筋力の増大に成功した[3]．しかし，アミノグリコシド系抗菌薬には聴覚毒性と腎毒性があるため，高用量を長期にわたり遺伝性疾患の患者に投与することは困難である．そこで安全でリードスルー活性の高い化合物の開発が行われている．PTC Therapeutics社が開発したリードスルー薬PTC124（ataluren®）[4]は米国でDMD患者を対象とした治験が実施されたが，残念ながら患者の臨床症状に有意な改善が認められなかったため，現在は開発が延期されている．

我が国でも，低分子化合物のスクリーニングにより独自のリードスルー薬の開発が行われている．さらに，アミノグリコシド系抗生物質であるネガマイシンを基本骨格として，抗菌活性とリードスルー活性を分離した誘導体の開発も進行中である．一方で，すでにMRSA治療薬として認可されているアルベカシンが比較的高いリードスルー活性を有することがわかり，DMDに対して日本で医師主導臨床治験が進行中である．

3）ミオスタチン阻害による筋量増大と筋再生の促進

ミオスタチンは骨格筋特異的に発現するTGF-βファミリー分子である．以前からヨーロッパでは筋肉量が2～3倍に増大した肉牛（Belgian blue, Piedmontese）や羊（Texel）などの家畜が知られていたが，こうした家畜のミオスタチン遺伝子を調べてみるといろいろな変異が発見された．さらに，2005年にはミオスタチン遺伝子変異を持つ男児も報告された．この男児は新生児の頃から筋肉がよく発達していて，5歳にして3 kgのダンベルを水平挙上できたという．このようにミオスタチンは骨格筋量を抑制的に調節していることが明らかになってきた．

*mdx*マウスにミオスタチン中和抗体を投与したところ，ジストロフィー病理変化と筋力が改善したことから[5]，ミオスタチン阻害療法は新たな筋ジストロフィー治療法として注目されるようになった．Weyth社はヒト化抗体MYO-029を開発し，Becker型筋ジストロフィー，肢帯型筋ジストロフィー，顔面肩甲上腕型筋ジストロフィー患者を対象として第2相治験を実施した．安全性は確認されたが，エンドポイントである徒手筋力テストや筋MRI検査で有意な改善が得られなかったことから，開発が断念された．

一方，bimagrumabはアクチビンのタイプII受容体に働く抗体医薬であり，ミオスタチンやアクチビンなどリガンドの結合を阻害し，これら因子からのシグナルを遮断することにより筋発達を刺激する[6]．ノバルティス社が共同開発しており，封入体筋炎の他，COPD，癌悪液質，サルコペニアの治療薬としても開発を進めている．

4）縁取り空胞を伴う遠位型ミオパチー（distal myopathy with rimmed vacuoles：DMRV）のシアル酸補充療法

DMRVは常染色体劣性遺伝疾患で原因遺伝子はGNE（UDP-N-acetylglucosamine 2-epimerase/N-acetylmannosamine kinase，シアル酸の合成を

触媒する酵素の1つ)で,最近はGNEミオパチーともよばれる.通常10歳代後半から30歳代後半に発症する.遠位筋,特に前脛骨筋が好んで侵され,大腿四頭筋は侵されにくい.徐々に筋萎縮が進行し,発症から平均12年で歩行不能となる.日本には300～400人程度の患者が存在すると予想される.モデルマウス研究により,シアル酸補充療法の有効性が明らかになっており[7],この研究成果を受けて,シアル酸補充療法は,日本では第1相,米国では第2相試験が行われている.

2. 福山型筋ジストロフィーの分子標的治療

1) ジストログリカノパチーの新たなメカニズム

福山型先天性筋ジストロフィー(Fukuyama congenital muscular dystrophy:FCMD)は1960年福山らにより発見された常染色体劣性遺伝疾患である.我が国の小児期筋ジストロフィーではDuchenne型の次に多く,日本人の約90人に1人が保因者とされる.日本に1,000～2,000人ほどの患者が存在すると推定され,日本人特有の疾患とされていたが,近年海外からの報告が相次いでいる.本症は重度の筋ジストロフィー病変とともに,多小脳回を基本とする高度の脳奇形(小多脳回)が共存し,さらに最近は近視,白内障,視神経低形成,網膜剝離などの眼症状も注目されている.すなわち,本症は遺伝子異常により骨格筋-眼-脳を中心に侵す一系統疾患である.

FCMDの疾患責任遺伝子であるフクチン遺伝子(*fukutin*, 9q31)は1998年に筆者らにより同定された.ほとんどのFCMD患者は,フクチン遺伝子の末端側の,蛋白質をコードしない3'非翻訳領域に「動く遺伝子」である約3千塩基長(3 kb)のSVA(Sine-VNTR-*Alu*)型レトロトランスポゾンの挿入型変異を認める[8].この変異は約100世代前,日本人祖先の1人に生じたとされるため,日本人の90人に1人が保因者で約3万出生に1人発症すると考えられている[8].

フクチン遺伝子が同定された後に,FCMDでは筋膜上の糖蛋白であるαジストログリカンの糖鎖に対する抗体の反応性が低いことが報告された.そして,糖転移酵素POMGnT1, POMT1/2がそれぞれ,FCMDの類縁疾患であるmuscle-eye-brain病, Walker Warburg症候群の原因遺伝子であることが次々と明らかにされた.これら患者の骨格筋では細胞膜と基底膜を繋ぐ糖蛋白α-ジストログリカンのO-マンノース型糖鎖修飾Siaa2-3Galb1-4GlcNAcb1-2Manに欠損があり,この糖鎖を介する細胞膜-基底膜間の結合が破綻するために重度の筋ジストロフィーが発症すると考えられるようになり,これらの疾患をαジストログリカノパチーと総称し新しい疾患概念ができた(図2A)[9].フクチン蛋白はゴルジ体に局在し,既知の糖転移酵素とのアミノ酸配列相同性よりαジストログリカン(αDG)の糖鎖修飾に関与する糖転移酵素ではないかと考えられているが,その機能を含め未知な点が多い.

ところで,ラミニン結合に関わる糖鎖として,Siaa2-3Galb1-4GlcNAcb1-2Manに加え,最近,O-マンノシル糖鎖にはリン酸基を介した側鎖構造があり,リン酸基より先の修飾もラミニン結合に必要であることが報告された(図2B)[10].この構造の合成にはLARGEが関与することが示されているが,興味深いことに,FCMD患者由来の細胞でもホスホジエステル結合を介した構造が欠如している.詳細な構造同定に加え,この修飾におけるフクチンの役割の解明が急がれる.また我々は,FKRP(fukutin-related protein)モデルマウスでもこのホスホジエステル結合を介した構造が欠如していること,さらには正常の肺や精巣組織でもαジストログリカンのリン酸基を介した側鎖構造が欠如しており,ラミニン結

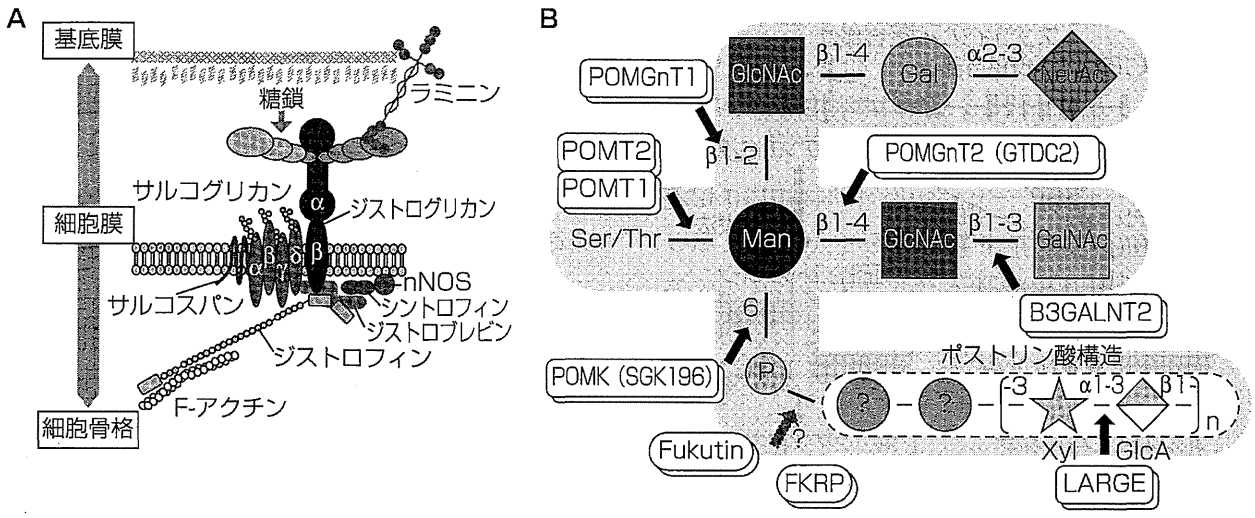

図2. 筋細胞膜のジストロフィン糖蛋白質複合体とαジストログリカン（αDG）の糖鎖修飾異常を発症要因とする疾患群「αジストログリカノパチー」

A　αジストログリカンはラミニンα2鎖とO型糖鎖を介して結合する．糖鎖修飾に異常をきたすと，ラミニンなどのリガンドとの結合能が低下し，αジストログリカノパチーを発症する．

B　ラミニン結合に関して，O-マンノース型糖鎖（Siaa2-3Galb1-4GlcNAcb1-2Man）とO-マンノシル糖鎖にリン酸基を介して修飾される側鎖構造が重要と考えられている．フクチンとLARGEはリン酸基より先の修飾に関与していると考えられる．

合能がないことを示し，この構造が正常組織でもラミニン結合能の決定因子であることを示した．

さらに，近年vitroでLARGEの酵素活性が明らかにされ，キシロースとグルクロン酸のリピートをつくる活性があることが示された．このキシロース-グルクロン酸リピートが天然のαジストログリカンに存在するかは不明であるが，少なくとも，キシロースはラミニン結合活性に必要である[11]．最近，ジストログリカン上のLARGEによるグリカン部分の伸長とその細胞外マトリックスリガンドに対する結合能の間に，直接的な相関関係があることが明らかにされた．LARGEグリカン反復配列が短いと，ジストロフィーの素因となる筋肉の機能不全などの様々な欠陥が生じる．さらに，臨床的な重症度の高い筋ジストロフィー患者ほど，LARGEグリカンの短縮の度合いが大きいことも明らかになった（図2B）[12]．

ポストリン酸糖鎖の構造はいまだに不明であるが，さらに最近，O-マンノースにつく別の側鎖としてPOMGnT2/b3GalNT2/POMKによって厳密に制御される修飾が明らかにされている（図2B）[13]．

2）FCMDはスプライシング異常症である

近年，我々はFCMDの根本的治療法につながる分子メカニズムと治療法を発見した[14]．フクチンは10個のエクソンと長い3'非翻訳領域（3'-UTR）をもつ．ほとんどのFCMD患者は，原因遺伝子の3'非翻訳領域にSVA型レトロトランスポゾン（以降SVA）の挿入を持つ．過去のデータではノザンハイブリダイザーション法では患者のフクチンmRNAは検出されなかった[7]．そこで今回我々は，フクチン内の全エクソン，SVA挿入配列，および3'-UTR領域の全域にわたる発現解析を再度検証し，対照と比較した．その結果，フクチンの5'側の翻訳領域部分，および3'-UTRのうちSVA挿入配列3'側の遺伝子発現は対照と患者間でほとんど変化がない一方，その配

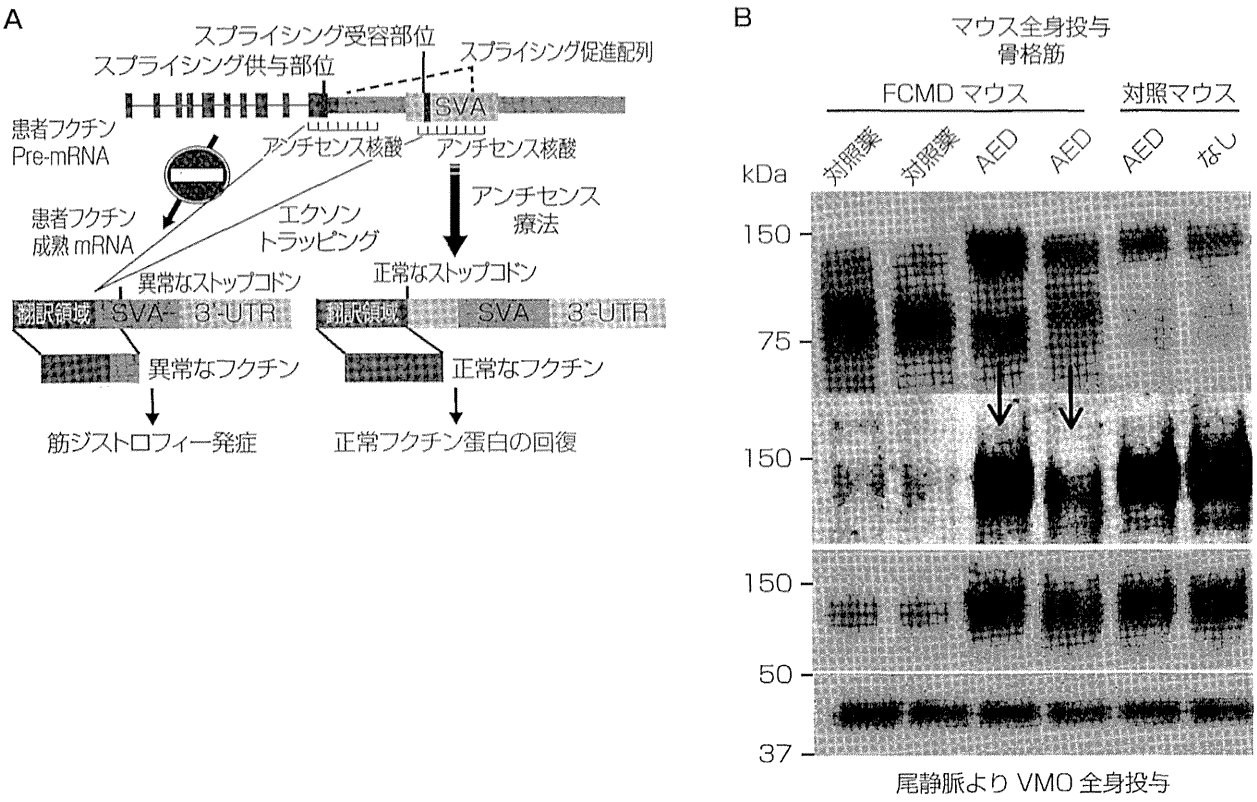

図 3. 福山型のアンチセンス治療

A FCMDのSVA型レトロトランスポゾン挿入によるエクソントラッピングがもたらすスプライシング異常とアンチセンス治療の構想

FCMDではSVA内の強力な3'側スプライシング受容部位により，最終エクソン内の潜在的ドナー部位が強力に活性化され，エクソントラップが起き，スプライシング異常を引き起こす．異常スプライシングを促進する配列に相補的なアンチセンス核酸を設計し，スプライシング配列をマスクすることにより異常スプライシングを阻止する．

B マウス骨格筋のウエスタンブロッティング．尾静脈よりAEDカクテルを全身投与．糖化型αジストログリカン（矢印）およびラミニン結合能が回復した．

列に挟まれる領域での遺伝子発現は患者でのみ激減していた．よって，患者のmRNAでは翻訳領域及びSVAの挿入の間のどこかでスプライシングが起きているのではないかと考え，発現の激減している配列をはさむ部分にPCRプライマーを設計し，患者及び対照のmRNA由来のcDNAを鋳型にPCRを行ったところ患者特異的に対照よりも短い遺伝子産物を検出した．この遺伝子産物の塩基配列の解析より，やはり患者ではフクチンmRNAが異常なスプライシングを受けていたことがわかった．

この異常スプライシングは，SVA挿入配列内に存在する強力なスプライシング受容部位が，蛋白質をコードする最終エクソン内の潜在的なスプライシング供与部位を新たに活性化すること（エクソントラッピング）が原因となっていた(図 3A)[14]．新たにスプライシング供与部位となった配列は，もともとは最終エクソン内に存在するために使われることのなかった，いわば眠っていたスプライシング供与部位であったのだが，SVAのエクソントラッピング機能により揺り起こされ，遺伝子の「切り取り」が生じた

のである．次に，この異常スプライシング由来の配列をもつコンストラクトを作成し，HeLa細胞へ導入し強制発現させたところ，スプライシング由来のフクチンの局在が，正常においてみられるゴルジ体局在から小胞体へ変化していた．これらより，FCMDはSVAのエクソントラップ機能がもたらすスプライシング異常症であることが証明された[14]．

3）FCMDに対するアンチセンス療法「エクソントラップ阻害療法」

SVAが挿入された患者のフクチンは，異常スプライシングさえ受けなければ，正常のフクチンをコードする正常なエクソン配列を体内に持っている．そこで，この異常スプライシングを阻止する目的で，異常スプライシングの標的配列に対し，アンチセンス核酸をpre-mRNAレベルで結合させ，正常なスプライシングに戻す，「アンチセンス療法」が有効ではないかと考えた（図3A）．そこで，これらの標的配列に対し有効なアンチセンス核酸を網羅的に設計し，様々な細胞系に投与しスプライシングの是正を検討し，3種のアンチセンス核酸のカクテル（AEDカクテルと命名）を選び出した．

次に，我々はビボモルフォリノ（octa-guanidine morpholino：VMO）というアンチセンス核酸を用い，AEDカクテルをモデル動物および患者細胞に投与し治療効果を検討した．患者筋芽細胞に対し，AEDカクテルを投与したところ，対照薬投与に比較し，糖鎖の回復を示唆する糖化型αDGの劇的な増加がみられた[14]．また尾静脈経由のモデルマウスへのAEDカクテル全身投与においても，Oマンノース型糖鎖の劇的な回復がみられた（図3B）[14]．最後に，患者由来筋芽細胞を使いAEDカクテル投与によるラミニン凝集アッセイを行った．患者筋芽細胞では筋管でのαDGの発現は激減している．しかし，AEDカクテル投与により，患者由来の筋管はαDGの糖鎖が正常レベルに回復し，正常と同程度の典型的なラミニンの凝集が観察された[14]．これらの結果はAEDカクテル投与により，筋管が機能的にも回復したことを示唆する．

また，ポストリン酸糖鎖不全モデルとして2種類の組織時期特異的フクチン欠損コンディショナルノックアウトマウスを樹立し，筋幹細胞/筋再生におけるポストリン酸糖鎖の重要な役割や，静脈投与によるAAV遺伝子治療により筋病変が回復することを示した[15]．

おわりに

筋ジストロフィーはかつてのように不治の病ではなくなりつつある．今回，我々が開発した方法は「エクソントラップ阻害療法」とでも命名でき，本邦FCMDの根本的分子標的治療に道を拓くものである[14]．また，Duchenne型と異なり，患者のほとんどが同じ変異なので，FCMDに対するアンチセンス療法は，日本のすべてのFCMDの患者を対象に同一の方法で行えるものであり有望である．国際治験中のDuchenne型エクソン52欠失は患者の10%であり，FCMD患者数をDuchenne型の1/3としても，日本での治療対象者は福山型の方が多いと思われる．今後，臨床試験の実現を目指したい．

福山型は我が国で初めて記載された疾患であり，患者数も多く，我が国の研究により，治療法開発を進めることは我々の責務であると考える．なお，我々が同定開発したフクチンの遺伝子検査は，2006年より健康保険適応となっていることを付記しておく．

著者のCOI（conflicts of interest）開示：戸田達史；研究費・助成金（大日本住友製薬）

文　献

1）Goemans NM, et al：Systemic administration of PRO051 in Duchenne's muscular dystrophy. N Engl J Med 364：1513–1522, 2011.

2) Cirak S, et al : Exon skipping and dystrophin restoration in patients with Duchenne muscular dystrophy after systemic phosphorodiamidate morpholino oligomer treatment : an open-label, phase 2, dose-escalation study. Lancet 378 : 595–605, 2011.
3) Barton-Davis ER, et al : Aminoglycoside antibiotics restore dystrophin function to skeletal muscles of mdx mice. J Clin Invest 104 : 375–381, 1999.
4) Welch EM, et al : PTC124 targets genetic disorders caused by nonsense mutations. Nature 447 : 87–91, 2007.
5) Bogdanovich S, et al : Functional improvement of dystrophic muscle by myostatin blockade. Nature 420 : 418–421, 2002.
6) Lach-Trifilieff E, et al : An antibody blocking activin type II receptors induces strong skeletal muscle hypertrophy and protects from atrophy. Mol Cell Biol 34 : 606–618, 2014.
7) Malicdan MC, et al : Prophylactic treatment with sialic acid metabolites precludes the development of the myopathic phenotype in the DMRV-hIBM mouse model. Nat Med 15 : 690–705, 2009.
8) Kobayashi K, et al : An ancient retrotransposal insertion causes Fukuyama-type congenital muscular dystrophy. Nature 394 : 388–392, 1998.
9) Kanagawa M, et al : The genetic and molecular basis of muscular dystrophy : roles of cell-matrix linkage in the pathogenesis. J Hum Genet 51 : 915–926, 2006.
10) Yoshida-Moriguchi T, et al : O-mannosyl phosphorylation of alpha-dystroglycan is required for laminin binding. Science 327 : 88–92, 2010.
11) Inamori K, et al : Dystroglycan function requires xylosyl- and glucuronyltransferase activities of LARGE. Science 335 : 93–96, 2012.
12) Goddeeris MM, et al : LARGE glycans on dystroglycan function as a tunable matrix scaffold to prevent dystrophy. Nature 503 : 136–140, 2013.
13) Yoshida-Moriguchi T, et al : SGK196 is a glycosylation-specific O-mannose kinase required for dystroglycan function. Science 341 : 896–899, 2013.
14) Taniguchi-Ikeda M, et al : Pathogenic exon-trapping by SVA retrotransposon and rescue in Fukuyama muscular dystrophy. Nature 478 : 127–131, 2011.
15) Kanagawa M, et al : Impaired viability of muscle precursor cells in muscular dystrophy with glycosylation defects and amelioration of its severe phenotype by limited gene expression. Hum Mol Genet 22 : 3003–3015, 2013.

福山型筋ジストロフィー　仕組みの解明 治療法開発

戸田達史
神戸大学大学院医学研究科　神経内科学／分子脳科学

デュシェンヌ型筋ジストロフィーの原因遺伝子としてジストロフィンが発見されて以来、この 20 年間で、40 種以上の筋ジス原因遺伝子が報告されている。我が国において、デュシェンヌ型に次いで多い小児期筋ジスである福山型先天性筋ジストロフィー（FCMD）は、先天性筋ジストロフィーに多小脳回などの脳奇形を伴う常染色体性劣性遺伝疾患であり、我々の９０人に１人が保因者である。1960 年に福山幸夫博士によって発見され、その約 40 年後の 1998 年に、我々によって、原因遺伝子フクチンが同定された。

福山型は、muscle-eye-brain 病(MEB)などと類似疾患とされる。我々は遠藤玉夫博士らとともに糖転移酵素 POMGnT1 の遺伝子が MEB 原因遺伝子であることを明らかにした。FCMD や MEB、Walker-Warburg(WWS)症候群、肢帯型 2I 型などに共通した病態として、αジストログリカンの糖鎖修飾異常が発見され、αジストログリカノパチーという新しい疾患概念が確立された。糖転移酵素の欠損によりαジストログリカンの糖鎖修飾が乱れ、ラミニンなどとの結合ができなくなり、脳奇形を伴う筋ジストロフィーが発症していると考えられている。

さらに近年、福山型筋ジストロフィーの根本的治療法につながる分子メカニズムと治療法を発見した。殆どの FCMD 患者は、フクチン遺伝子の 3’ 非翻訳領域に約 3kb の SVA 型レトロトランスポゾンの挿入変異を持つ。我々は、FCMD が SVA の挿入により誘導される「スプライシング異常症」であることを見いだした。さらに異常スプライシングを阻止するため、スプライシング配列を標的とするアンチセンス核酸を設計し、患者由来細胞に導入、及び FCMD モデルマウスに筋注ならびに全身投与した結果、患者由来細胞において正常のフクチンが回復し、またモデルマウスにおいて正常フクチンの回復、αジストログリカンの糖鎖修飾及びラミニン結合能の回復が確認された。SVA のエクソントラッピング機能はヒトの疾患や進化に関与しており、FCMD に対しては初の根治療法実現の可能性が示唆される（エクソントラップ阻害療法）。

本講演では、福山型筋ジストロフィーの臨床、遺伝子、病態、分子標的治療などを概観する。

Available online at www.sciencedirect.com

ScienceDirect

Neuromuscular Disorders 25 (2015) 60–69

www.elsevier.com/locate/nmd

Congenital myasthenic syndrome in Japan: Ethnically unique mutations in muscle nicotinic acetylcholine receptor subunits

Yoshiteru Azuma [a,b], Tomohiko Nakata [a,b], Motoki Tanaka [c], Xin-Ming Shen [d], Mikako Ito [a], Satoshi Iwata [a], Tatsuya Okuno [a], Yoshiko Nomura [e], Naoki Ando [f], Keiko Ishigaki [g], Bisei Ohkawara [a], Akio Masuda [a], Jun Natsume [b], Seiji Kojima [b], Masahiro Sokabe [c], Kinji Ohno [a,*]

[a] *Division of Neurogenetics, Center for Neurological Diseases and Cancer, Nagoya University Graduate School of Medicine, Nagoya, Japan*
[b] *Department of Pediatrics, Nagoya University Graduate School of Medicine, Nagoya, Japan*
[c] *Department of Physiology, Nagoya University Graduate School of Medicine, Nagoya, Japan*
[d] *Department of Neurology, Mayo Clinic, Rochester, MN, USA*
[e] *Segawa Neurological Clinic for Children, Tokyo, Japan*
[f] *Department of Pediatrics, Nagoya City University Graduate School of Medicine, Nagoya, Japan*
[g] *Department of Pediatrics, Tokyo Women's Medical University, Tokyo, Japan*

Received 29 May 2014; received in revised form 9 August 2014; accepted 3 September 2014

Abstract

Congenital myasthenic syndromes (CMS) are caused by mutations in genes expressed at the neuromuscular junction. Most CMS patients have been reported in Western and Middle Eastern countries, and only four patients with *COLQ* mutations have been reported in Japan. We here report six mutations in acetylcholine receptor (AChR) subunit genes in five Japanese patients. Five mutations are novel, and one mutation is shared with a European American patient but with a different haplotype. Among the observed mutations, p.Thr284Pro (p.Thr264Pro according to the legacy annotation) in the epsilon subunit causes a slow-channel CMS. Five other mutations in the delta and epsilon subunits are splice site, frameshift, null, or missense mutations causing endplate AChR deficiency. We also found a heteroallelic p.Met465Thr in the beta subunit in another patient. p.Met465Thr, however, was likely to be polymorphism, because single channel recordings showed mild shortening of channel openings without affecting cell surface expression of AChR, and the minor allelic frequency of p.Met465Thr was 5.1% in the Japanese population. Lack of shared mutant alleles between the Japanese and the other patients suggests that most mutations described here are ethnically unique or *de novo* in each family.

Keywords: Congenital myasthenic syndromes; Acetylcholine receptor; Slow channel syndrome; Fast channel syndrome; Endplate acetylcholine receptor deficiency

1. Introduction

Acetylcholine released from the nerve terminal binds to muscle nicotinic acetylcholine receptor (AChR) at the motor endplate. AChR is clustered at the neuromuscular junction (NMJ) by binding to rapsyn with a stoichiometry of rapsyn to AChR of 1:1 to 2:1 [1]. AChR clustering is mediated by neural agrin that is released from the nerve terminal [2]. In early embryonic development, AChR clustering is also mediated by Wnt ligands [3,4]. Embryonic AChR is composed of α, β, δ, and γ subunits with a stoichiometry of $\alpha_2\beta\delta\gamma$. After birth, the ε subunit is substituted for the γ subunit, generating $\alpha_2\beta\delta\varepsilon$-AChR.

Congenital myasthenic syndromes (CMS) are heterogeneous disorders caused by mutations in genes expressed at the NMJ [5]. They are characterized by fatigable muscle weakness, variable muscle atrophy, and sometimes dysmorphic features. CMS mutations have been reported in 19 genes, with most mutations in *CHRNA1*, *CHRNB1*, *CHNRD*, and *CHNRE* encoding the AChR α, β, δ, and ε subunits, respectively. These mutations fall into three subsets: i) slow-channel CMS (SCCMS), in which the open time of AChR is abnormally prolonged; ii) fast-channel CMS (FCCMS), in which the open time of AChR is abnormally brief; and iii) endplate AChR deficiency. SCCMS is caused by a gain-of-function mutation and is dominantly inherited with variable penetrance [6]. In contrast, FCCMS and endplate AChR deficiency are caused by loss-of-function mutations on both alleles, and are recessively

* Corresponding author. Division of Neurogenetics, Center for Neurological Disease and Cancer, Nagoya University Graduate School of Medicine, 65 Tsurumai, Showa-ku, Nagoya 466-8550, Japan. Tel.: +81 52 744 2446; fax: +81 52 744 2449.
E-mail address: ohnok@med.nagoya-u.ac.jp (K. Ohno).

http://dx.doi.org/10.1016/j.nmd.2014.09.002
0960-8966/

inherited. Low-expressor mutations of the AChR ε subunit are partly compensated for by expression of the embryonic AChR γ subunit, whereas the other AChR subunits have no substituting subunits. Accordingly, null and frameshift mutations are frequently detected in *CHRNE*, but not in the other subunit genes.

More than 500 patients with CMS have been reported in Western and Middle Eastern countries, whereas only four Japanese CMS patients carrying five mutations in *COLQ* encoding collagen Q that anchors acetylcholinesterase (AChE) at the NMJ have been reported by us [7,8]. Among the more than 450 CMS mutations in 19 disease genes registered in the Human Gene Mutation Database (http://www.hgmd.org), two likely have founder effects: p.Asn88Lys in *RAPSN* [9–11] and c.1124_1127dupTGCC in *DOK7* [12], whereas the others are private mutations occurring in a single or a small number of unrelated families. We here report five Japanese CMS patients with six mutations in the AChR subunit genes. We show that all the ten mutations in *COLQ*, *CHRND*, and *CHRNE* in Japanese patients are ethnically unique, which indicates that most CMS mutations arose *de novo* in recent human history or in each family.

2. Materials and methods

2.1. Ethical approval

All the human studies were approved by the institutional review boards of Nagoya University Graduate School of Medicine, Mayo Clinic, Segawa Neurological Clinic for Children, Nagoya City University, and Tokyo Women's Medical University. Appropriate written informed consent was obtained from all the patients and family members.

2.2. Mutation analysis and splicing analysis

Genomic DNA was isolated from peripheral blood with QIAamp Blood Kit (QIAGEN). We directly sequenced all exons with their flanking noncoding regions of *CHRNE*, *CHRNA1*, *CHRNB1*, and *CHRND* in this order with CEQ 8000 (Beckman Coulter). To look for large-scale DNA rearrangements in patient (Pt.) 4, we performed mate-pair sequencing of the whole genome using SOLiD4 (Life Technologies). The mate-pair library was made to span ~2 kb genomic segments according to the manufacturer's protocols. A total of 14.9 Gb of reads were mapped to human genome GRCh37/hg19 with the mapping efficiency of 89% using CLC Genomics Workbench (CLC Bio). All the reads mapped to *CHRNE* were visually scrutinized using Integrative Genome Browser (Broad Institute). Total RNA was isolated from biopsied muscle that was obtained for histopathological diagnostic purposes using RNeasy mini kit (QIAGEN). cDNA was synthesized with ReverTra Ace (Toyobo) and Oligo(dT) Primer (Life Technologies).

2.3. Expression of AChR subunit genes in HEK293 cells

Human α, β, δ, and ε subunit cDNAs were cloned into the CMV-based vector pRBG4 for expression in HEK293 cells [13]. The identified mutations were engineered into wild-type AChR subunit cDNAs in pRBG4 using the QuikChange site-directed mutagenesis kit (Stratagene). Presence of each mutation and absence of unwanted artifacts were confirmed by sequencing the entire inserts. HEK293 cells were transfected with pRBG4-α, -β, -δ, -ε, and pcDNA3.1-EGFP at a ratio of 2:1:1:1:1 using FuGENE 6 transfection reagent (Promega). After 48 hrs, cells were incubated with α-bungarotoxin Alexa Flour 647 (Life Technologies) (1:200) in PBS for 1 hr. Signals were observed under an Olympus BX60 fluorescence microscope. The cells were trypsinized, washed with PBS, and resuspended in PBS. The total number of α-bungarotoxin-binding sites on the cell surface and EGFP was determined by the FACSCalibur system (BD Biosciences).

2.4. Single channel recordings

HEK293 cells were transfected with pRBG4-α, -β, -δ, and -ε, and pEGFP-N1 at a ratio of 2:1:1:1:1, using FuGENE 6. Recordings were obtained at 24 hrs after transfection in the cell-attached configuration at a membrane potential of –80 mV at 22 °C and with bath and pipette solutions containing (in mM): KCl, 142; NaCl, 5.4; CaCl2, 1.8; MgCl2, 1.7; HEPES, 10, pH 7.4. Single-channel currents were recorded using an Axopatch 200B amplifier (Axon Instruments) at a bandwidth of 50 kHz, digitized at 5-μs intervals using Digidata 1322A (Axon Instruments) and recorded to a hard disk using the program Clampex 8.2 (Axon Instruments). Recordings obtained with ACh at 1 μM or less were analyzed at a uniform bandwidth of 10–11.7 kHz with dead time of 15.3–17.9 μs imposed. Recordings obtained with ACh at 10 μM or more were analyzed with dead time at 25 μs at 10 kHz with TAC software (Ver. x4.0.9, Bruxton). Dwell-time histograms were plotted on a logarithmic abscissa and fitted by the sum of exponentials by maximum likelihood, as previously reported [14].

3. Results

3.1. Clinical features

All Pts. had an abnormal decremental response to repetitive nerve stimulation, and no anti-AChR and anti-MuSK antibodies. Clinical features and repetitive nerve stimulation results are summarized in Table 1.

Pt. 1 (13 y.o., male) had eyelid ptosis since age six months and a positive edrophonium test. Clinical features were previously reported in a local journal [15]. Steroid pulse therapy at ages four and five years and thymectomy at age six years had no effect. Combined use of distigmine 3 mg/day and pyridostigmine 180 mg/day enabled him to sit in a chair without assistance at age 13 years. Biopsy of deltoid muscle at age eleven years showed marked AChR deficiency by fluorescent staining with α-bungarotoxin and simplified endplates by electron microscopy.

Pt. 2 (26 y.o., female) had nasal obstruction since birth and eyelid ptosis since age one month. She had a positive edrophonium test and was thought to have myasthenia gravis. Cholinesterase inhibitors were mildly effective. She has ophthamoparesis, and is able to walk but is unable to run.

Table 1
Clinical features of six patients.

Pt.	Sex	Age	Onset	Consanguinity	Repetitive N. stimulation[a]	Drug[b]
1	M	13 y	6 m	–	Accessory N., 60%; Ulnar N., 53%	Distigmine 3 mg + pyridostigmine 180 mg, effective; 3,4-DAP 40 mg, mildly effective
2	F	26 y	1 m	+	Ulnar N., 80%	Pyridostigmine 150–180 mg, mildly effective
3	F	38 y	1 y	–	Ulnar N., 81%	Pyridostigmine 90–160 mg, moderately effective
4	F	6 y	2 y	–	Median N., 60%; Ulnar N., 68%	Pyridostigmine 90 mg + 3,4-DAP 30 mg, mildly effective; ephedrine 25 mg, effective
5	M	26 y	1 m	+	Ulnar N., 76%	Pyridostigmine 135 mg, moderately effective
6	M	11 y	Birth	–	Median N., 35%; Ulnar N., 31%	Prednisolone 35 mg *dieb. alt.*, effective

[a] Repetitive N. stimulation, repetitive nerve stimulation at 2–3 Hz. Relative amplitudes of the 5th CMAP are indicated. [b] Simultaneous prescription is indicated by "+".

Pt. 3 (38 y.o., female) had ptosis at age one year and was diagnosed to have myasthenia gravis at age seven years. Since then, she has been taking cholinesterase inhibitors and prednisolone, which seemed to help but could not climb steps after age 19 years.

Pt. 4 (6 y.o., female) walked alone at age 18 months, but since age two years she had repeated episodes of generalized muscle weakness that lasted about a week, especially when having a common cold. She could walk alone but was positive for a Gowers' sign. Cholinesterase inhibitors were moderately effective. Neurological examination of the mother detected no abnormality. The father was asymptomatic according to the mother, but was not examined by us. Clinical features were previously reported as patient 4 in a local journal [16].

Pt. 5 (26 y.o., male) had feeding difficulty at age one month and had eyelid ptosis since age five months. He has weak facial muscles and is unable to run. At age seven years, he had generalized muscle weakness during an upper respiratory infection. The edrophonium test was positive.

Pt. 6 (11 y.o., male) had repeated respiratory distress and respiratory infection during infancy. He walked alone at age one year, but was noticed to walk slowly at age five years with frequent falling episodes. Rest for a short time improved his walking, but there was no diurnal fluctuation of the symptoms. Intravenous administration of edrophonium chloride ameliorated walking difficulty, but long-acting cholinesterase inhibitors had no effect.

3.2. Mutation analysis

We directly sequenced AChR subunit genes in Pts. 1–6, and identified six mutations in *CHRND* and *CHRNE*, as well as a polymorphism in *CHRNB1* (Table 2). In this study, approved nucleotide and amino acid positions are used instead of the legacy annotation, in which nucleotide and amino acid positions start from the initiation sites of mature peptides.

Pt. 1 was compound heterozygous for c.1372-1G>A at the 3′ end of intron 11 of *CHRND* and c.127C>T predicting p.Arg44Trp at the extracellular domain of the δ subunit (Fig. 1A). cDNA extracted from biopsied muscle revealed that a newly generated 'ag' dinucleotide that was one nucleotide downstream of the native 'ag' was used as a splice acceptor site (Fig. 1B), which predicted p.Glu458Argfs*20 in the long cytoplasmic loop of the δ subunit (Fig. 1A). Pt. 2 was homozygous for c.655_665del predicting p.Gly219Argfs*7 in the extracellular domain of the ε subunit (Fig. 1A). Pt. 3 was heterozygous for p.Tyr262Ter in the M1 transmembrane domain of the ε subunit (Fig. 1A). Pt. 4 was heterozygous for p.Thr284Pro in the M2 transmembrane domain of the ε subunit (Fig. 1A). Pt. 5 was homozygous for p.Leu304Arg in the short extracellular link between the M2 and M3 transmembrane domains of the ε subunit (Fig. 1A). Pt. 6 was heterozygous for p.Met465Thr close to the C-terminal end of the long cytoplasmic loop connecting the M3 and M4 transmembrane domains of AChR β subunit (Fig. 1A).

Table 2
Six mutations and one polymorphism identified in AChR subunit genes.

Pt.	Gene	Nucleotide change[c]	Amino-acid change[c]	Legacy annotation[d]	Phenotypic consequence
1	*CHRND*	c.1372-1G>A	δp.Glu458Argfs*20	δE437fs	AChR deficiency
	CHRND	c.127C>T	δp.Arg44Trp	δR23W	AChR deficiency
2[a]	*CHRNE*	c.655_665del	εp.Gly219Argfs*7	εG199fs	AChR deficiency
3[b]	*CHRNE*	c.786C>G	εp.Tyr262Ter	εY242X	AChR deficiency
4	*CHRNE*	c.850A>C	εp.Thr284Pro	εT264P	SCCMS
5[a]	*CHRNE*	c.911T>G	εp.Leu304Arg	εL284R	AChR deficiency
6	*CHRNB1*	c.1394T>C	εp.Met465Thr	βM442T	~50% shortening of AChR openings

[a] Patient is homozygous for the mutation.
[b] A mutation on another allele remains unidentified.
[c] Nucleotide and amino acid positions start from the translational start sites.
[d] In legacy annotation, nucleotide and amino acid positions start from the initiation sites of mature peptides, which are 69 nt. (23 amino acids), 63 nt. (21 amino acids), and 60 nt. (20 amino acids) downstream of the translational start sites of *CHRNB1*, *CHRND*, and *CHRNE*, respectively.

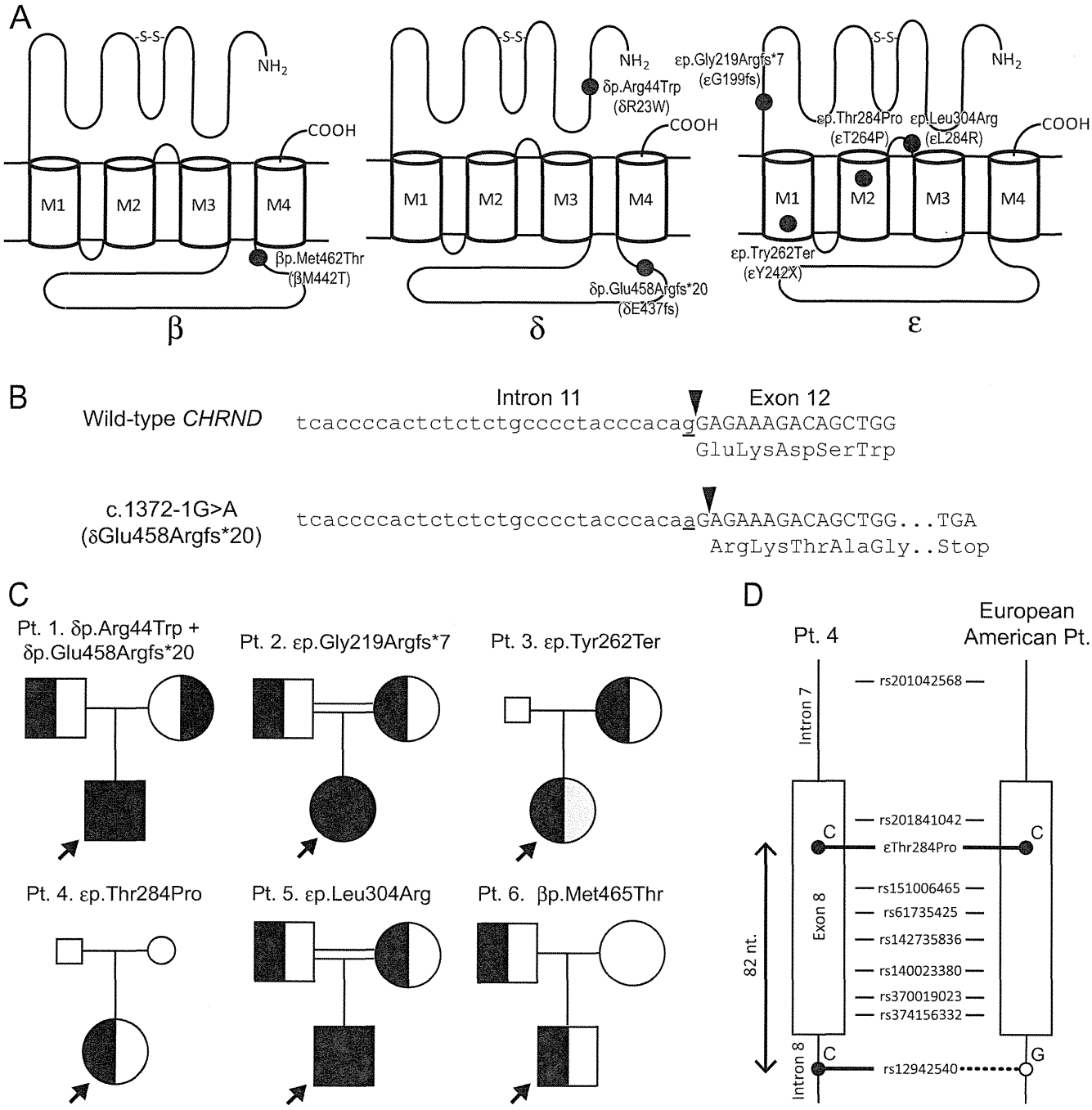

Fig. 1. Six mutations and a single polymorphism in AChR subunit genes identified in six CMS patients. (A) Positions of six mutations and a polymorphism. M1-M4, the first to fourth transmembrane domains. The M2 domains form a channel pore of AChR. (B) RT-PCR of biopsied muscle of Pt. 1 reveals that c.1372-1G>A (underlined) shifts a splice acceptor site (arrowheads) one nucleotide downstream, which predicts a shift in the reading frame (δp.Glu458Argfs*20). (C) Pedigree analyses of the mutations. Patients are indicated by arrows. Full and half shaded symbols represent homozygous and heterozygous mutations, respectively. Gray half shaded symbols represent that the individuals are predicted to carry a heterozygous mutation, the identity of which, however, has not been identified. Small symbols indicate that DNA is not available. (D) Haplotype analysis of εp.Thr284Pro in Pt. 4 and the previously reported European American Pt [7]. Both patients carry discordant nucleotides at rs12942540, which is 82 nt. downstream of the mutation.

δp.Arg44Trp (rs55868108) in Pt. 1 was previously reported in one of five healthy controls, but its ethnic origin was not documented [17]. δp.Arg44Trp, however, is not observed in the 1000 genome project (http://www.1000genomes.org/) or in the human gene variation database (HGVD), which collates SNPs in a large cohort of Japanese individuals (http://www.genome.med.kyoto-u.ac.jp/SnpDB/) [18]. As indicated below, functional analysis disclosed that δp.Arg44Trp

Table 3
Open intervals and bursts of wild-type and mutant AChR expressed on HEK cells.

	Open intervals		Bursts	
	Wild-type	βp.Met465Thr	Wild-type	βp.Met465Thr
τ_1 (ms)	0.037 ± 0.0033[a]	0.022[b]	0.036 ± 0.0017[c]	0.039 ± 0.006[d]
(a_1)	(0.17 ± 0.022)	(0.18)	(0.24 ± 0.021)	(0.18 ± 0.034)
τ_2 (ms)	0.31 ± 0.050	0.16 ± 0.017[e]	0.47 ± 0.059	0.16 ± 0.037[f]
(a_2)	(0.27 ± 0.038)	(0.23 ± 0.031)	(0.21 ± 0.027)	(0.23 ± 0.010)
τ_3 (ms)	1.35 ± 0.051	0.98 ± 0.034	3.31 ± 0.12	1.93 ± 0.085
(a_3)	(0.67 ± 0.042)	(0.78 ± 0.028)	(0.58 ± 0.038)	(0.82 ± 0.034)

Twenty-one wild-type and seven mutant patches were analyzed. Time constants, τ_n, and fractional areas, a_n, for each component are presented with mean ± SEM. ACh concentration was 50–100 nM.
[a–f] Not detected at 12, 6, 3, 5, 1, and 3 patches, respectively.
Final band widths were 11.7 and 10 kHz for wild-type and mutant AChRs, respectively.

significantly reduces cell surface expression of AChR and is unlikely to be polymorphism.

p.Met465Thr (rs201776800) in Pt. 6 was observed in eight alleles in eight Japanese individuals in the 1000 genome project with a minor allelic frequency (MAF) of 0.004, as well as in 119 alleles in a cohort of 1170 Japanese individuals in HGVD with a MAF of 0.051. Although p.Met465Thr was likely to be a polymorphism according to the high MAFs in the Japanese, we scrutinized functional consequences of p.Met465Thr in this study.

3.3. *εp.Gly219Argfs*7, εp.Tyr262Ter, and δp.Glu458Argfs*20 are predicted to compromise AChR expression*

Among the six mutations, εp.Gly219Argfs*7 in Pt. 2 and εp.Tyr262Ter in Pt. 3 were predicted to produce truncated ε subunits. We previously reported that truncation mutations in the εsubunit lead to expression of the embryonic $\alpha_2\beta\delta\gamma$-AChR at the patient's endplates and the patients have endplate AChR deficiency [19–21]. The ε mutations in Pts. 2 and 3 were thus predicted to cause AChR deficiency.

δp.Glu458Argfs*20 in Pt. 1 was predicted to generate a truncated δ subunit that cannot be incorporated into mature AChR. The phenotype of Pt. 1 is thus determined by δp.Arg44Trp on the other allele, which causes AChR deficiency as indicated below.

3.4. *εp.Thr284Pro is an established slow-channel mutation without shared haplotype with a European American patient*

εp.Thr284Pro in the M2 domain of the ε subunit was identical to the first characterized slow-channel mutation reported in a patient of Swiss and Turkish descent [22]. We asked if the mutation in Pt. 4 derived from the same founder allele as the first reported patient. Therefore we sequenced exon 8 and its flanking intronic regions where nine SNPs were located (Fig. 1C). This revealed that the mutant allele in the Japanese patient had 'C', whereas the mutant allele in the European American patient had 'G' at rs12942540 in intron 8, which was located 82 nt. downstream of εp.Thr284Pro. Accordingly, εp.Thr284Pro in both patients is likely to have occurred independently in two ethnic groups.

3.5. *δp.Arg44Trp and εp.Leu304Arg, but not βp.Met465Thr, decrease cell surface expression of AChR in transfected HEK293 cells*

We next analyzed the effects of AChR expression of the remaining three mutations of δp.Arg44Trp, εp.Leu304Arg and βp.Met465Thr. We introduced wild-type or mutant α, β, δ, and ε subunit cDNAs along with EGFP cDNA into HEK293 cells (Fig. 2A), and measured cell surface expression of AChR detected by Alexa 647-labeled α-bungarotoxin using FACS. Expression of βp.Met465Thr-AChR was similar to that of wild-type AChR, whereas δp.Arg44Trp and εp.Leu304Arg markedly attenuated the cell surface expression of AChR (Figs. 2B and C). Accordingly, δp.Arg44Trp and εp.Leu304Arg cause endplate AChR deficiency.

3.6. *βp.Met465Thr mildly shortens channel opening events, but not as much as the other established fast channel mutations*

As βp.Met465Thr-AChR was efficiently expressed on HEK293 cells, we next recorded opening and closing of single AChR channels at limiting low concentrations of ACh by the patch clamp method (Fig. 3A). We found that the major burst duration (τ_3) was decreased from 3.31 ms to 1.93 ms (58.3%) in βp.Met465Thr-AChR (Table 3), while the conductance of βp.Met465Thr-AChR was normal. Distributions of opening probabilities of the clusters generated by 10 μM or greater concentrations of ACh made single peaks for both wild-type and mutant AChRs. Thus, βMet465Thr mildly shortens the channel openings but does not cause a mode switching in the kinetics of the receptor activation, which is seen in other FCCMS mutations [23,24].

3.7. *A recessive mutation on the other allele in Pt. 3 remains unidentified*

Functional prediction and characterization of the six mutations indicated that εp.Thr284Pro in Pt. 4 was a dominant slow-channel mutation [22], whereas the other five mutations in Pts. 1, 2, 3, and 5 were recessive loss-of-function mutations. The mutations in Pts. 1, 2, and 5 were biallelic, whereas a mutation was detected only on a single allele in Pt. 3 (Fig. 1C).

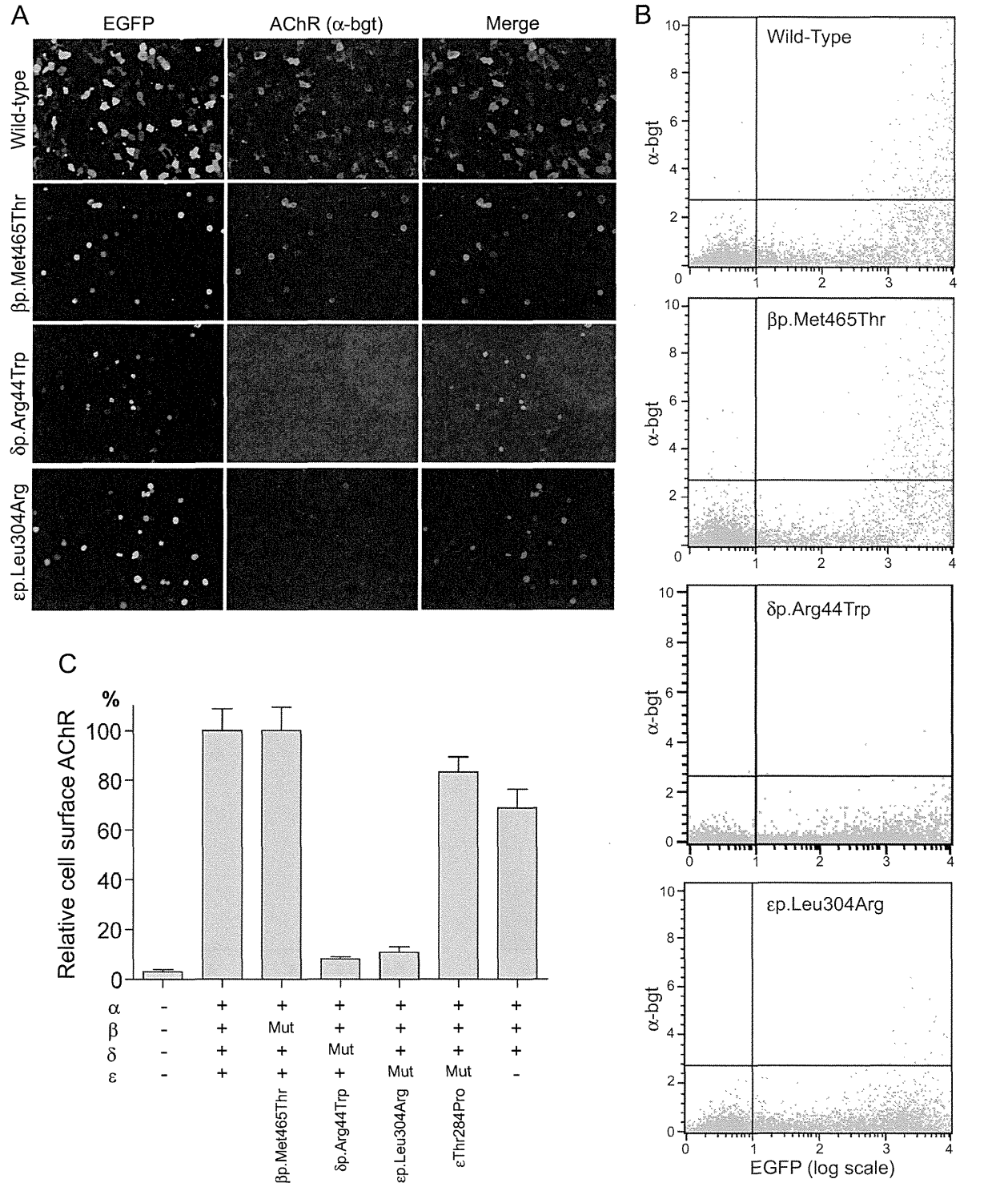

Fig. 2. Quantification of cell surface expression of wild-type and mutant AChRs on HEK293 cells. (A) HEK293 cells are transfected with wild-type or mutant AChR subunit cDNAs along with EGFP cDNA. Only transfected cells have EGFP signals and AChRs that are visualized with Alexa 647-labeled α-bungarotoxin (bgt). εp.Leu304Arg-AChR has less signals for AChRs compared to wild-type and βp.Met465Thr-AChRs. (B) Representative FACS profiles of EGFP and Alexa 647-labeled α-bgt. Both axes are shown in arbitrary units. The number of cells fractioned into the upper right quadrant is counted as AChR-positive cells. (C) Ratios of AChR-positive cells (the upper right quadrant) divided by EGFP-positive cells (the lower right quadrant). δp.Arg44Trp and εp.Leu304Arg markedly decrease AChR expression, whereas βp.Met465Thr and εp.Thr284Pro have no effect on AChR expression. ε-deficient $\alpha_2\beta\delta_2$-AChR are expressed at ~70% of wild-type, as we reported previously [21]. Mut, a mutant AChR subunit. Mean and SE are indicated ($n = 12$).

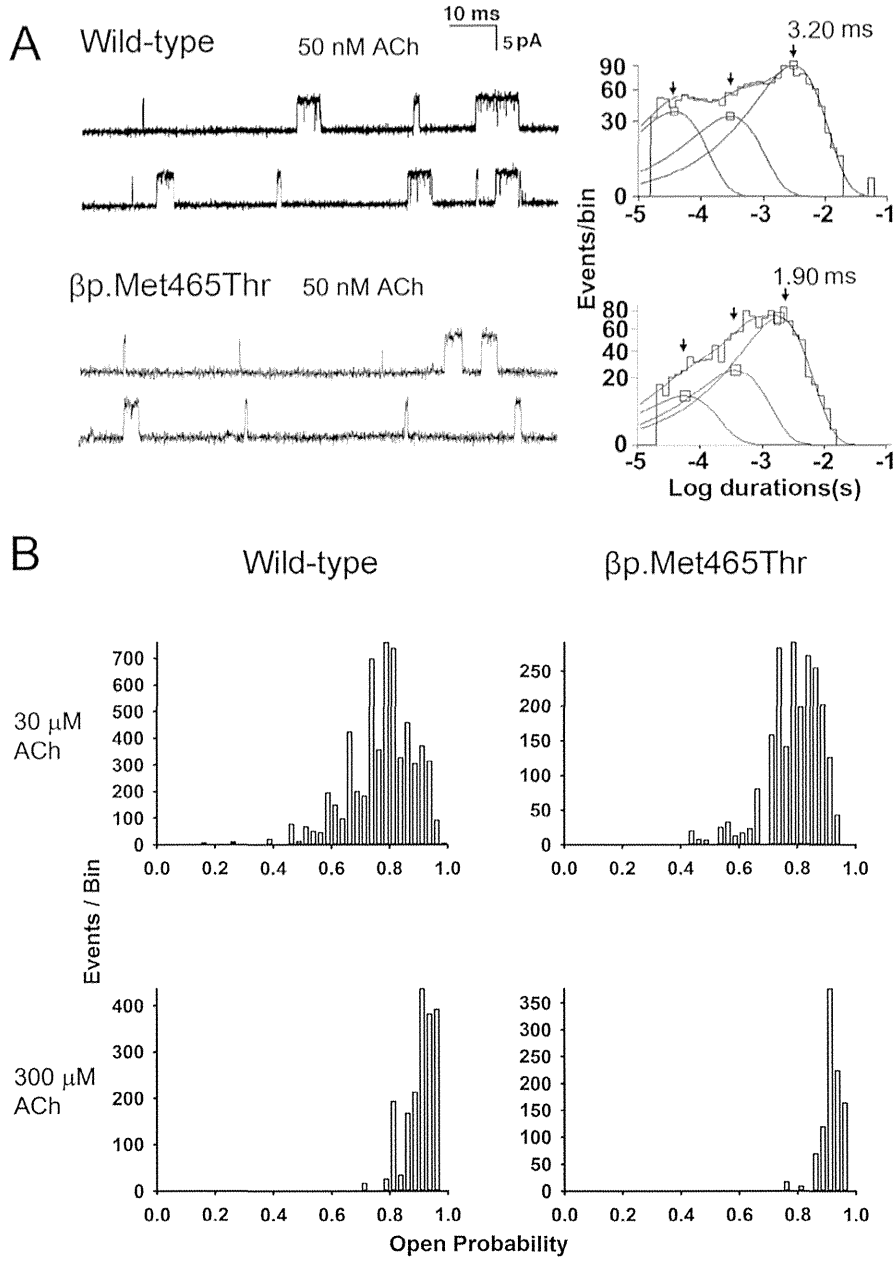

Fig. 3. Single channel currents of wild-type and mutant AChRs on HEK293 cells. (A) Left: Representative channel openings shown as upward deflections. Right: Burst duration histograms fitted to the sum of exponentials. Arrows indicate mean durations of dominant burst components. (B) Distribution of open probabilities from individual clusters obtained at the indicated ACh concentrations. Note that both wild-type and mutant AChRs make a single peak.

We scrutinized all exonic nucleotides in *CHRNE* in Pt. 3 by bidirectional sequencing, but detected none. We therefore hypothesized that a mutation on the other alleles was either a promoter mutation, a splice-site mutation disrupting a deep intronic splicing *cis*-element, or a large-scale DNA rearrangement. Sequencing of ~1 kb upstream of the translation initiation sites, however, revealed no mutation. We further analyzed genomic DNA by mate-pair sequencing of the whole genome. A total of 57 reads were mapped to *CHRNE*. Visual inspection of these reads, however, failed to detect any large-scale DNA rearrangements or any mutations. A recessive mutation on the other allele in *CHRNE* in Pt. 3 thus remains unidentified. We also analyzed 18 other CMS-causing genes using the mate-pair sequencing data in Pt. 3. As the mate-pair sequencing was for detecting a large-scale DNA rearrangement, the 18 genes were covered by only 10,116 reads. Although the coverage was not high enough for detecting SNVs, no candidate mutations were detected in Pt. 3.

Table 4
Fifteen previously reported FCCMS mutations and the currently analyzed βp.Met462Thr polymorphism.

Mutation	Burst duration (ms)			Expression	Domain	Reference
	Wild-type	Mutant	Ratio	(%)		
αp.Val152Leu (αV132L)	3.31	0.50	0.151	135	Extracellular domain of α	[25]
αp.Val208Met (αV188M)	3.31	0.68	0.205	90	Extracellular domain of α	[26]
αp.Phe276Leu (αF256L)	3.62	0.30	0.083	102	M2 domain of α	[27]
αp.Val305Ile (αV285I)	2.99	0.34	0.114	116	M3 domain of α	[28]
δp.Leu63Pro (δL42P)	3.31	0.18	0.054	37	Extracellular domain of δ	[14]
δp.Glu80Lys (δE59K)	5.06	2.75	0.543	62	Extracellular domain of δ	[29]
δp.Pro271Gln (δP250Q)	3.31	1.54	0.465	60	M1 domain of δ	[30]
εp.Thr58Lys (εT38K)	5.86	0.06	0.010	78	Extracellular domain of ε	[31]
εp.Trp75Arg (εW55R)	3.31	0.37	0.112	86	Extracellular domain of ε	[32]
εp.Pro141Leu (εP121L)	2.99	0.45	0.151	102	Extracellular domain of ε	[13]
εp.Asp195Asn (εD175N)	2.13	0.49	0.230	117[b]	Extracellular domain of ε	[33]
εp.Asn202Tyr (εN182Y)	2.13	0.65	0.305	117[b]	Extracellular domain of ε	[33]
εp.Ser433_Glu438dup (ε1254ins18)	2.80	1.01	0.361	47	Long cytoplasmic loop of ε	[23]
εp.Ala431Pro (εA411P)	n.a.[a]	n.a.[a]	n.a.[a]	31	Long cytoplasmic loop of ε	[24]
εp.Asn456del (εN436del)	3.31	1.24	0.375	51	Long cytoplasmic loop of ε	[34]
βp.Met462Thr (βM442T)	3.31	1.93	0.583	99	Long cytoplasmic loop of β	Current study

A major component of burst durations of wild-type and mutant AChRs expressed in HEK293 cells is indicated. Cell surface expression in HEK293 cells is normalized to that of wild-type. Channel openings are elicited by 50–100 nM ACh. Mutations in parentheses are legacy annotations used in original reports.

[a] Detailed ion channel kinetics are analyzed using a hidden Markov model, but burst durations are not indicated.

[b] Cell surface expression of recombinant AChR is not indicated, and the expression ratio is calculated from α-bungarotoxin binding sites of control and patient endplates.

4. Discussion

We identified six mutations in AChR subunit genes in five Japanese patients with CMS. We initially assumed that βp.Met465Thr in Pt. 6 was a mild fast-channel mutation. However, expansion of the SNP database later disclosed that βp.Met465Thr is a polymorphism that is frequently observed in the Japanese population. Fifteen previously reported FCCMS mutations shorten burst durations to 22.6 ± 16.1% of wild-type (mean and SD; range 1.0%–54.3%) (Table 4). A FCCMS mutation, δp.Glu80Lys (δE59K), decreases burst durations to 54.3% of wild-type [29], which is similar to 58.3% observed in the current βp.Met465Thr polymorphism. However, in contrast to βp.Met465Thr, δp.Glu80Lys reduces cell surface expression of AChR to 62% of wild-type [29]. Similarly, δp.Pro271Gln (δP250Q) mildly reduces burst durations to 46.5% of wild-type, but again, unlike βp.Met465Thr, this mutation reduces cell surface expression of AChR to 60% of wild-type [30]. A plot of normalized burst durations and normalized cell surface expressions suggests that a mean burst duration of less than ~30% causes FCCMS even when it does not affect the cell surface expression of AChR (Fig. 4). In contrast, a mean burst duration of between ~30% and ~60% causes FCCMS when the mutation reduces the cell surface expression of AChR to ~60% or less (Fig. 4). However, as no individual is homozygous for βp.Met465Thr or carries a null mutation on the other allele, pathogenicity of βp.Met465Thr in the absence of a normal *CHRND* on the other allele still remains unknown.

δp.Arg44Trp is close to the N-terminal end of the extracellular region (Fig. 5). We previously reported that a similar εp.Arg40Trp also causes AChR deficiency [35]. The specific function of this region, however, is not well dissected. εp.Leu304Arg is in the short extracellular link between the M2 and M3 transmembrane domains (Fig. 5). The functions of this link are not well characterized. In this link, only αp.Ser289Ile (αS269I) is reported in SCCMS [38]. βp.Met465Thr is located close to the C-terminal end of the long cytoplasmic loop that links the M3 and M4 transmembrane domains (Fig. 5). Interestingly, three FCCMS mutations in the long cytoplasmic loop are clustered close to the C-terminal end of the ε subunit [23,24,34,36,37], and similarly destabilize the channel open state. Two FCCMS mutations in this region, εp.Ser433_Glu438dup (ε1254ins18) [23] and εp.Ala431Pro (εA411P) [24], disrupt the fidelity of gating and result in unstable channel kinetics. In addition, another FCCMS

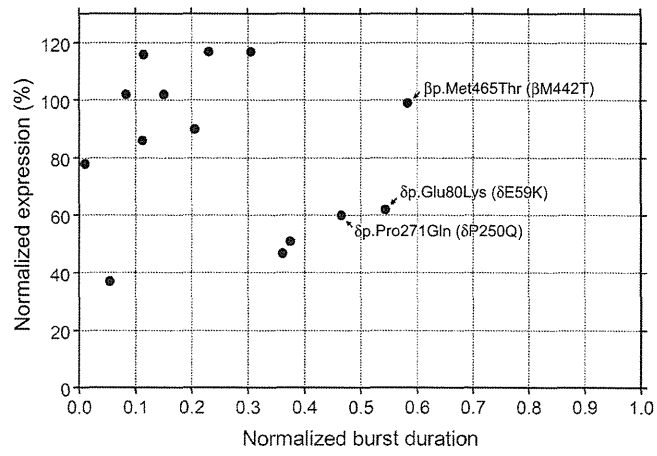

Fig. 4. Normalized burst durations and normalized cell surface expressions of previously reported FCCMS mutations and the currently analyzed βp.Met462Thr polymorphism shown in Table 4. Arrows point to mutations and a polymorphism that are addressed in the discussion.